The Astronomical Journal, 126:1402–1414, 2003 September

THE CFHT OPEN STAR CLUSTER SURVEY. IV. TWO RICH, YOUNG OPEN STAR CLUSTERS: NGC 2168 (M35) AND NGC 2323 (M50)

Jasonjot Singh Kalirai,[1,2] Gregory G. Fahlman,[3] Harvey B. Richer,[1] and Paolo Ventura[4]

Received 2003 May 2; accepted 2003 May 28

ABSTRACT

We continue our study of rich Galactic clusters by presenting deep CCD observations of both NGC 2168 (M35) and NGC 2323 (M50). Both clusters are found to be rich (NGC 2168 contains at least 1000 stars brighter than $V = 22$, and NGC 2323 contains ~2100 stars brighter than our photometric limit of $V \sim 23$) and young (NGC 2168 age = 180 Myr and for NGC 2323 age = 130 Myr). The color-magnitude diagrams for the clusters exhibit clear main sequences stretching over 14 mag in the (V, $B-V$)-plane. Comparing these long main sequences with those of earlier clusters in the survey, as well as with the Hyades, has allowed for accurate distances to be established for each cluster (for NGC 2168 $d = 912^{+70}_{-65}$ pc and for NGC 2323 $d = 1000^{+81}_{-75}$ pc). Analysis of the luminosity and mass functions suggests that, despite their young ages, both clusters are somewhat dynamically relaxed, exhibiting signs of mass segregation. This is especially interesting in the case of NGC 2323, which has an age of only 1.3 times the dynamical relaxation time. The present photometry is also deep enough to detect all of the white dwarfs in both clusters. We discuss some interesting candidates that may be the remnants of quite massive ($M \geq 5\ M_{\odot}$) progenitor stars. The white dwarf cooling age of NGC 2168 is found to be in good agreement with the main-sequence turnoff age. These objects are potentially very important for setting constraints on the white dwarf initial-final mass relationship and the upper mass limit for white dwarf production.

Key words: open clusters and associations: individual (NGC 2168, NGC 2323) — stars: evolution — stars: luminosity function, mass function — white dwarfs

1. INTRODUCTION

The Canada-France-Hawaii Telescope (CFHT) Open Star Cluster Survey (Kalirai et al. 2001a, hereafter Paper I) is a large imaging program primarily designed to catalog hundreds of white dwarf stars in open star clusters. Spectroscopic observations of these white dwarfs with 8 m class telescopes (currently underway) will yield important observational constraints on both the white dwarf initial-final mass relationship and the upper mass limit to white dwarf production. In addition to studying white dwarfs, the survey has motivated several other investigations. For example, we are using a grid of new theoretical isochrones, calculated especially for this project, both to determine the ages of the clusters and to confront the theoretical predictions with observational data. With accurate photometry down to $V = 24$ for the richest clusters, the quality of the data has made these tests much more reliable than in the past. The long, tightly constrained main sequences of the clusters are also being fitted to the Hyades and Pleiades main sequences to determine accurate distances. Dynamical effects are being investigated by using updated mass-luminosity relations to convert luminosity functions into mass functions. The wide-field photometry for individual clusters has also allowed us to study the cluster extent, stellar density profiles, mass segregation, and binary star counts. Other studies concerned with proper motions, variable stars, radial velocities, brown dwarfs, synthetic color-magnitude diagram (CMD) tests, blue stragglers, binary white dwarfs, and Galactic disk star distributions are currently being undertaken through collaborations. Detailed results on the first cluster we examined, NGC 6819, are published in Kalirai et al. (2001b, hereafter Paper II). The second cluster we looked at, NGC 2099, is described in Kalirai et al. (2001c, hereafter Paper III). This work, Paper IV in our series, presents the study of the two young clusters NGC 2168 (M35) and NGC 2323 (M50).

Our deep V, $B-V$ photometry covers a larger areal extent for each cluster than previous studies, presents the tightest main sequence to date, and extends the photometry to bluer stars and therefore detects the faintest white dwarfs. Our primary goals in this work are to better constrain the ages of and distances to each cluster, investigate the cluster luminosity and mass functions for dynamical effects, and catalog potential white dwarfs for future spectroscopic observations.

Perhaps the most important motivation for the study of young open star clusters is to set constraints on the initial mass function (IMF). Unlike the general field population, clusters provide samples of stars that contain the same metallicity and are of the same age. For young clusters in which dynamics have not yet altered the stellar population, the present-day observed mass function is a close approximation of the IMF. NGC 2168 and NGC 2323 are good candidates for these studies.

NGC 2168 (M35) is a well-studied cluster since its rich stellar population has long been recognized (Smart 1925; Trumpler 1930; Ebbighausen 1942; Meurers & Schwarz

[1] Department of Physics and Astronomy, 6224 Agricultural Road, University of British Columbia, Vancouver, BC V6T 1Z1, Canada; jkalirai@physics.ubc.ca, richer@astro.ubc.ca.

[2] Visiting Astronomer, Canada-France-Hawaii Telescope, operated by the National Research Council of Canada, the Centre National de la Recherche Scientifique de France, and the University of Hawaii.

[3] National Research Council of Canada, Herzberg Institute of Astrophysics, 5071 West Saanich Road, RR5, Victoria, BC V9E 2E7, Canada; Greg.Fahlman@nrc.gc.ca.

[4] Osservatorio Astronomico di Roma, Sede di Monteporzio, Via Frascati 33, I-00040 Monteporzio Catone, Italy; paolo@coma.mporzio.astro.it.

1960). The most comprehensive of these early studies, that of Ebbighausen (1942), detected 150 stars down to a photovisual magnitude of 12.0. This study presented both the first CMD (actually plotting m_{bol} vs. log T_{eff}) and luminosity function for NGC 2168. Thirty years later, Cudworth (1971) used photographic plates dating back to 1916 to measure proper motions of 763 stars in the region of NGC 2168 (513 confirmed cluster members). He extended the cluster CMD down to $V \sim 14$.

Preliminary dynamical studies of stars in the region of NGC 2168 were motivated by Galactic structure studies. The density gradients near the anticenter of the Galaxy were shown to be significantly steeper than other directions in the solar neighborhood (Hersperger 1973; Topaktas 1975), and therefore they indicated anisotropies in the disk of the Milky Way.

NGC 2168 is an anticenter cluster in the plane of the disk ($l = 186^\circ 58'$, $b = 2^\circ 18'$) (B1950), and thus was mapped out in these three-color (*RGU*) studies. However, the first significant study of dynamics within NGC 2168 did not occur until 1986 when McNamara & Sekiguchi (1986a) investigated velocity dispersions in the cluster. They observed mass segregation and proposed a model for dynamical evolution in the cluster. In a separate effort, McNamara & Sekiguchi (1986b) also extended the CMD down to $V \sim 15$ and improved the photometric precision and calibration over previous studies (which were based on the photoelectric work of Hoag et al. 1961). The dynamical mass within the central 3.75 pc of NGC 2168 was estimated by Leonard & Merritt (1989) to be in the range of 1600–3200 $M_\odot$. This measurement used two-component velocity dispersion profiles (from the 61 yr epoch difference between photographic plates) to estimate the cluster potential.

The first CCD photometry for NGC 2168 was that of Sung & Bessell (1999), who determined the age, reddening, distance, metallicity, and minimum binary fraction. Their data extended the cluster photometry to $V \sim 20$. Even more recently, the WIYN Open Star Cluster Study has looked at both the metallicity (Deliyannis & Steinhauer 2001; Deliyannis, Barrado y Navascués, & Stauffer 2000) and the CMD (von Hippel et al. 2000, 2002) for NGC 2168 and drawn comparisons between this cluster and the Pleiades. Finally, Barrado y Navascués, Deliyannis, & Stauffer (2001b) and Barrado y Navascués et al. (1998, 2001b) have presented a very detailed investigation of stars ranging from close to the turnoff to the hydrogen burning limit in NGC 2168.

With so many studies of its population, the key cluster parameters of NGC 2168 (reddening, distance, and age) have been refined many times in the literature as observations have improved. We summarize these in Table 1. The best-fit values are those from the recent work of Barrado y Navascués et al. (2001a). Unlike NGC 2168, previous work on NGC 2323 (M50) has been very limited. Although several independent investigations of the cluster exist, they are mostly limited to observations of only a few stars. This is surprising considering that the cluster is smaller in angular size, richer in stellar population, and younger in age than

TABLE 1
SUMMARY OF PUBLISHED CLUSTER PARAMETERS FOR NGC 2168 AND NGC 2323

Year	Reddening [$E(B-V)$]	Distance (pc)	Age (Myr)	Type	Reference
NGC 2168:					
1930	...	840	...	Photographic	1
1938	...	740	...	Photographic	2
1961	0.23	870	...	...	3
1961	0.23	871	...	Photoelectric/photographic	4
1971	0.23	870	70–100	Photographic	5
1973	0.17	871	20–40	Photographic	6
1992	0.26–0.44	725	85	Photoelectric	7
1999	0.255	832	200	CCD	8
2000	0.3	731	100	CCD	9
2000	0.198	809	160	CCD	10
2001	...	832	175	CCD	11
2002	0.20	805	150	CCD	12
2003	...	912	180	CCD	13
NGC 2323:					
1930	...	780–860	...	Photographic	1
1930	...	500–800	...	Photographic	14
1931	...	675	...	Photographic	15
1935	...	520	...	Photographic	16
1941	0.30	1210	...	Photographic	17
1961	0.20–0.26	1170	...	Photoelectric	4
1969	...	...	60	Photographic	18
1983	0.33	995	140	Photographic	19
1998	0.25	931	100	Photoelectric	20
2003	...	1000	130	CCD	13

REFERENCES.—(1) Trumpler 1930; (2) Cuffey 1938; (3) Johnson et al. 1961; (4) Hoag et al. 1961; (5) Becker & Fenkart 1971; (6) Vidal 1973; (7) Sung & Lee 1992; (8) Sung & Bessell 1999; (9) von Hippel et al. 2000; (10) Sarrazine et al. 2000; (11) Barrado y Navascués et al. 2001a; (12) Deliyannis et al. 2003; (13) This work; (14) Shapley 1930; (15) Collinder 1931; (16) Rieke 1935; (17) Cuffey 1941; (18) Barbaro et al. 1969; (19) Mostafa 1983; (20) Claria et al. 1998.

NGC 2168. Early photographic and photoelectric studies of NGC 2323 found distances that varied by over a factor of 2: Trumpler (1930), 780–860 pc; Shapley (1930), 500–800 pc; Collinder (1931), 675 pc; Rieke (1935), 520 pc; Cuffey (1941), 1210 pc; Hoag et al. (1961), 1170 pc; and Mostafa et al. (1983), 995 pc. The first age determinations for the cluster varied by similar factors: Barbaro, Dallaporta, & Fabris (1969), 60 Myr, and Mostafa et al. (1983), 140 Myr. More recently, Claria, Piatti, & Lapasset (1998) presented *UBV* photoelectric measurements of 109 probable members of the cluster. This study, which has a limiting magnitude of $V \sim 14$, established $E(B-V) = 0.25$, $(m - M)_V = 10.62$ ($d = 940$ pc), and age $= 100 \pm 20$ Myr (from fitting the Bertelli et al. 1994 isochrones with mass loss and moderate overshooting). No previous CCD studies of this cluster were found in the literature. The present photometry detects $\sim$10 times as many cluster members as all previous studies combined.

We will first present the data and briefly discuss the photometry and calibration in § 2. In §§ 3 and 4 we present the CMDs for each cluster and fit isochrones to the data. This allows us to determine the age of each cluster and also investigate the quality of the fits. In § 5 we discuss dynamical effects in both clusters and compute the luminosity and mass functions. Finally, we present analysis of white dwarfs in NGC 2168 and NGC 2323 in § 6 and conclude this study in § 7.

2. OBSERVATIONS AND DATA REDUCTION

As with other clusters in the CFHT Open Star Cluster Survey, the data were obtained during a three-night observing run in 1999 October. All observations were obtained at the CFHT through standard V and B filters with the CFH12K mosaic camera, which has a $42' \times 28'$ field of view. NGC 2168 was imaged during night 3 of the run and NGC 2323 during night 1 (short exposures to get the photometry of giants were acquired at a later date). For NGC 2168, two 5 minute exposures were obtained in each color; however, only one was usable. This was combined with individual 50, 10, and 1 s exposures to complete the photometry. For NGC 2323, the photometry from single exposures of 300, 50, 10, and 1 s in each color was combined to produce a catalog of magnitudes and colors. The seeing conditions during the observations of NGC 2168 were $1\farcs15$ and the air mass was 1.60. For NGC 2323, the seeing was $0\farcs85$ and the air mass was 1.18.

The data were processed (flat-field, bias, and dark corrected) and combined using the FITS Large Images Processing Software (J.-C. Cuillandre 2001, private communication) as described in § 3 of Paper I. More then 53 flats and 13 bias frames were observed during the run.

We reduced the data using a preliminary version of the TERAPIX photometry routine PSFex (Point Spread Function Extractor; E. Bertin 2000, private communication). We used a separate, variable point-spread function for each CCD in the mosaic. Some features of PSFex are described in § 4 of Paper I.

Calibration was addressed by separately observing Landolt standard fields SA-92 and SA-95 (Landolt 1992) during the observing run. A total of 92 calibration stars (different configurations of exposure times, filters, and air masses) were used to calibrate the NGC 2168 data. For NGC 2323, 130 calibration stars were used (see Tables 2 and 3 in Paper I). Comparison of the aperture photometry of these stars with the PSFex photometry yielded the transformation equations required to calibrate the data (see §§ 5.1 and 5.2 of Paper I). The uncertainty in the zero points used for the calibration is estimated to be $\sim$0.018 in V and $\sim$0.017 in B. The air-mass coefficients are 0.087 ± 0.012 in V and 0.160 ± 0.006 in B, in good agreement with the CFHT estimations of 0.10 and 0.17, respectively. The color terms were averaged over the three-night observing run and are in agreement with the nominal CFHT estimates in the V filter and are slightly lower for the B filter.

The final errors in the photometry are found to be less than 0.01 mag for stars with $V < 19$ and up to 0.2 mag for the faintest ($V \sim 23$) stars.

3. THE NGC 2168 AND NGC 2323 COLOR-MAGNITUDE DIAGRAMS

Figures 1 and 2 present photometric CMDs for both NGC 2168 and NGC 2323. The panels on the left show all objects measured with PSFex, whereas the panels on the right depict only those objects with a stellarity index $\geq$0.50. This SExtractor image morphology parameter (Bertin & Arnouts 1996) uses a robust procedure to estimate source resolution, and we have shown in the past (Papers II and III) that this cut is effective in removing faint blue galaxies and other image defects. Clearly, the fainter parts of the CMDs in the right panels are much cleaner than those in the left panels. Some potential white dwarf candidates are also brought out in the faint blue end of the CMDs.

The CMD for NGC 2168 (Figure 1) shows a rich main sequence extending from $V \sim 8.5$ to $V \sim 22.5$. One potential cluster red giant is also seen at $V = 8.48$, $B-V = 1.32$ and can be used to constrain the age of the cluster through fitting of the blue loop. Although it is centrally located in the cluster, this object is only given a 56% probability as a cluster member in the proper-motion analysis by McNamara & Sekiguchi (1986a). The main sequence presented here is tighter than any of the previous studies on this cluster. This photometry is deep enough to detect the faintest white dwarfs in the cluster. These are believed to have originated from quite massive progenitors. The "clump" of objects near $V \sim 21.5$, $B-V \sim 0$ most likely represents the end of the white dwarf cooling sequence in this young cluster. This will be investigated further in § 6. The wall of stars bluer (or fainter) than the cluster main sequence is the background disk star population. With a Galactic latitude of only $\sim 2^\circ$, NGC 2168 resides very close to the plane of the Milky Way. Within our $40'$ diameter for the cluster field (one direction is cutoff at $28'$ by the CFH12K mosaic) we have detected many field stars that overlap with cluster members on the faint main sequence. The vertical feature in the CMD to the red of the cluster main sequence (at $14 \leq V \leq 17.5$, $B-V \sim 1.3$) may represent distant giant stars in the disk. This is smeared out in V because of the distance spread along the line of sight. The defined field does not encompass the entire radial extent of NGC 2168.

For NGC 2323, the CMD (Fig. 2) again shows a rich, long main sequence extending from the tip of the turnoff at $V \sim 8$ down to $V \sim 23$ at the limit of our data. As mentioned in § 1, the previous best study of this cluster, the photoelectric effort of Claria et al. (1998), detected only 109 cluster members brighter than $V \sim 14$. The SExtractor-

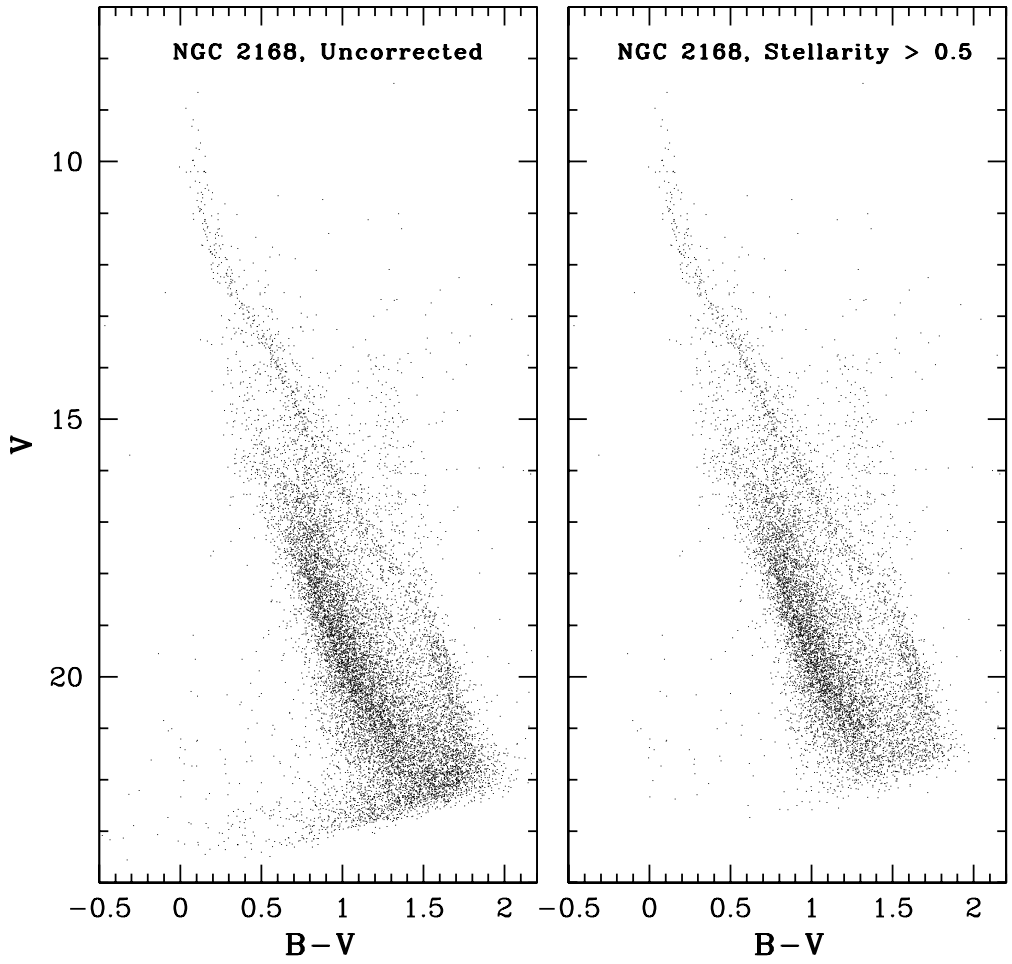

FIG. 1.—NGC 2168 CMD clearly shows a well-populated main sequence stretching from $V = 9$ to $V \sim 22.5$. After eliminating faint blue galaxies and other image defects with a 0.50 stellarity cut (*right*), some potential white dwarfs are seen at $V = 21.5$, $B-V = 0$.

cleaned CMD (Fig. 2, *right*) again shows several potential white dwarfs scattered in the faint blue end of the diagram.

3.1. *Cluster Reddening, Distance, and Metallicity*

As summarized in Table 1, several previous measurements of both the reddening and distance of NGC 2168 and NGC 2323 are available in the literature. We adopt reddening values from these studies and recompute the distances by comparing the cluster main sequences to the Hyades fiducial (de Bruijne, Hoogerwerf, & de Zeeuw 2001). Since there is minimal scatter in the main sequences for these clusters, there is almost no ambiguity in the distance determination. For NGC 2168, we adopt $E(B-V) = 0.20$ from the recent five-color (*UBVRI*) photometry by Sarrazine et al. (2000). The metallicity of NGC 2168 is known because of the high-resolution spectroscopic effort of Barrado y Navascués et al. (2001a), who find [Fe/H] $= -0.21 \pm 0.10$ ($Z \sim 0.01$). Other previous CCD studies (e.g., Sung & Bessell 1999) have also found subsolar metallicities for NGC 2168, using less robust techniques. To compare the Hyades sequence to NGC 2168, we first shift our CMD by $+0.09$ mag in $B-V$ to account for the $\Delta Z \sim 0.014$ metallicity difference (Hyades is given as $Z = 0.024$). The corresponding best-fit distance modulus is found to be $(m - M)_0 = 9.80 \pm 0.16$, which gives $d = 912 \pm 6570$ pc. The extinction has been corrected by using $A_V = 3.1E(B-V)$. This distance estimate is slightly greater than previous values for NGC 2168 (see Table 1); however, it is more precise because of the quality of the CMD.

For NGC 2323, we adopt a reddening value of $E(B-V) = 0.22$, which is an average of the recent Claria et al. (1998) study and the robust effort of Hoag et al. (1961). Although no detailed spectroscopic abundance analysis is published for NGC 2323, photometric investigations (e.g., Claria et al. 1998) have found that solar metallicity models best reproduce the observed cluster main sequence. We shift the CMD by $+0.03$ mag in $B-V$ to account for the $\Delta Z \sim 0.004$ metallicity difference and find that the best-fit distance modulus for NGC 2323 is $(m - M)_0 = 10.00 \pm 0.17$, which gives $d = 1000^{+81}_{-75}$ pc. As Table 1 shows, this distance is in good agreement with the most recent studies of NGC 2323

The uncertainties in the distances for these clusters are computed using a method identical to that used for NGC 2099 in Paper III. Briefly, the final uncertainty in the true distance modulus combines four individual uncertainties and accounts for correlations between them. These are (1) a scale factor translation from the $B-V$ axis to the V axis to account for the reddening uncertainty, (2) an estimated main-sequence fitting uncertainty at a fixed reddening value, (3) the error in the extinction, $\Delta_{A_V} = 3.1\Delta_{E(B-V)}$, and (4) the color uncertainty due to an estimated metallicity

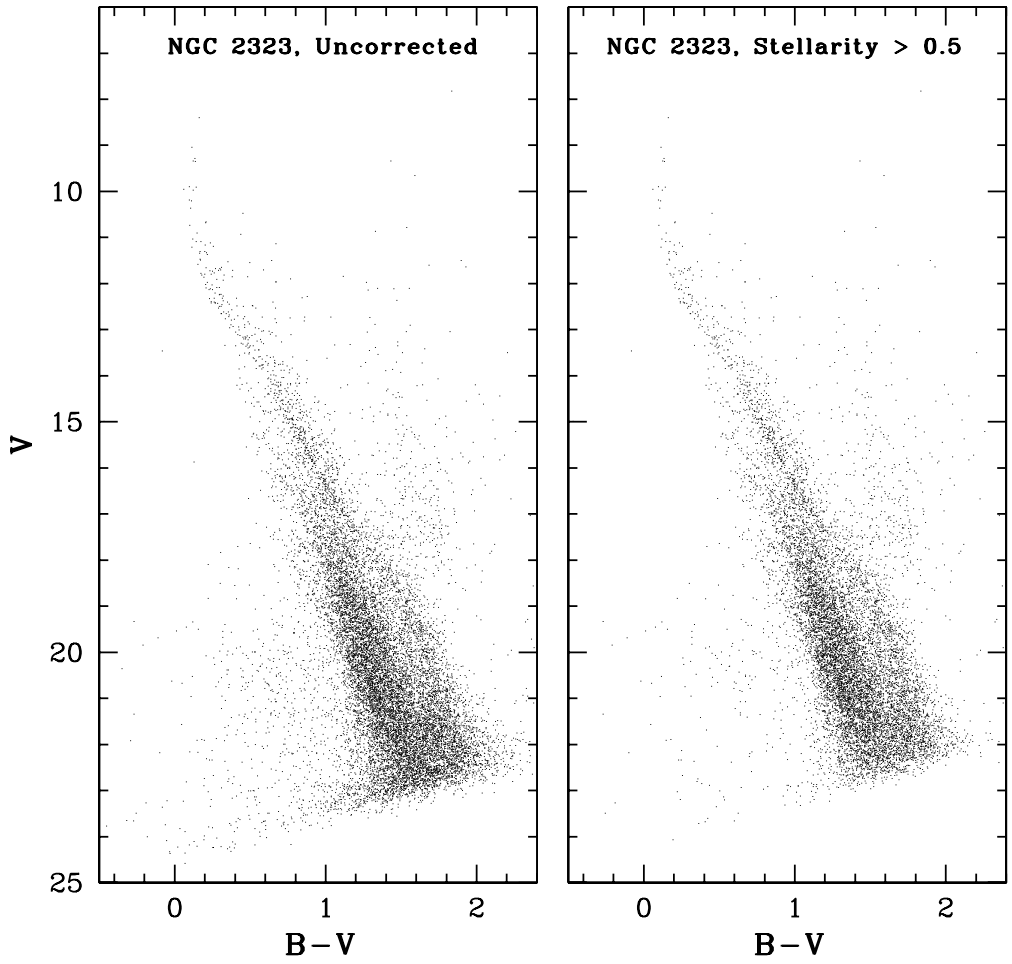

FIG. 2.—NGC 2323 CMD clearly shows a well-populated main sequence stretching from $V = 8$ to $V \sim 23$. After eliminating faint blue galaxies and other image defects with a 0.50 stellarity cut (*right*), some potential white dwarfs are seen scattered in the faint blue end of the CMD.

uncertainty, Δ_Z. Paper III describes the details of how these terms were combined.

4. THEORETICAL COMPARISONS

As with earlier clusters in the survey, we are using a new set of theoretical isochrones to compare the observations with theory. This set of models was computed especially for the CFHT Open Star Cluster Survey by the group at the Rome Observatory (P. Ventura and F. D'Antona). Section 5.2 of Paper II and § 3.4 of Paper III provide a description of the models. Here we present only a small summary and refer the readers to the earlier papers for more insight. A description of the stellar evolution code that was used to build the tracks is given in Ventura et al. (1998). Convective core overshooting is treated by means of an exponential decay of turbulent velocity out of the formal convective borders, and the convective flux has been evaluated according to the full spectrum of turbulence theory prescriptions (Canuto & Mazzitelli 1992). The Bessell, Castelli, & Plez (1998) conversions are used to convert luminosities to magnitudes and temperatures to colors. The lower main sequence ($M \lesssim 0.7\ M_\odot$) has been calculated by adopting NextGen atmosphere models (Hauschildt, Allard, & Baron 1999).

Figure 3 shows two panels with the best-fit isochrones for NGC 2168. For the core-overshooting model shown in the left panel, we find an age of 180 Myr. This is essentially identical to the 175 Myr value found by Barrado y Navascués et al. (2001a) and very close to the 150 Myr value found by von Hippel et al. (2002). There is a potential red giant star at $M_V = -1.94$, $(B-V)_0 = 1.21$, which helps constrain the location of the blue loop. This star [as well as a turnoff star located at $M_V = -1.76$, $(B-V)_0 = -0.09$] falls directly under the line that is used to draw the isochrone on the figure and is therefore difficult to see. We have increased the point size of all stars with $M_V \leq 0$ to help visualize the data. A non-overshooting model (*right*) is also shown, and this gives an age of 130 Myr. The ζ value in the figures represents the free parameter that specifies the *e*-folding distance of the exponential decay of turbulent velocities (Ventura et al. 1998).

The isochrone reproduces the general shape of the main sequence very nicely. Near the turnoff, the model correctly falls on the blue edge of the observed sequence, which is free of binary contamination. Models of ages 160–200 Myr in the overshooting case also provide acceptable fits to the observed cluster sequence. For the lower main sequence ($M_V \gtrsim 8$), we were not able to compute nongray atmospheres for this metallicity. We therefore overplot the lower main sequence from a solar metallicity ($Z = 0.02$) model,

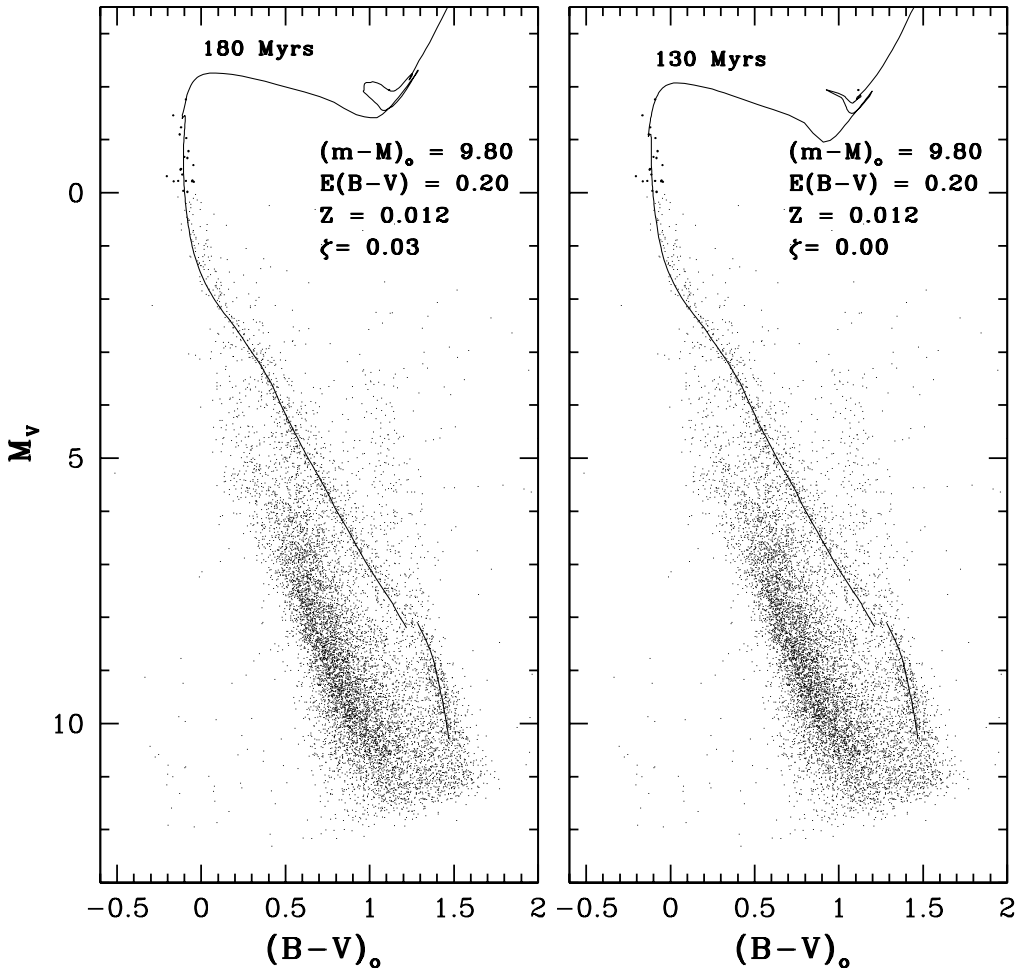

FIG. 3.—*Left*: Best-fit isochrones for NGC 2168 (age = 180 Myr), based on a core-overshooting model. *Right*: An equivalent fit obtained by using a non-overshooting model of 130 Myr. The discontinuity at $M_V = 8.2$ represents the limit to which we presently have nongray atmosphere models for this metallicity ($Z = 0.012$). Fainter than this magnitude, we plot our solar-metallicity isochrones. The metallicity difference causes a small shift between the colors of the two models; however, this does not take away from the excellent agreement on the lower main sequence between this model and the data. See § 4 for a discussion of these results. Note that the points representing stars with $M_V \leq 0$ have been made slightly larger and bolder for comparison purposes.

and therefore a discontinuity is seen in the CMD. A small color shift [of approximately $\Delta(B-V) = 0.06$] is needed to correct for the metallicity of the cluster. Such a shift would move the lower main sequence blueward, but not by an amount that would produce a poor fit.

Figure 4 shows isochrone comparisons for NGC 2323. The age, using a core-overshooting model (*left*) is found to be 120–140 Myr. The solar metallicity isochrone fits the observed main sequence and turnoff well. As in the case of the similar metallicity clusters NGC 6819 and NGC 2099, the lower main sequence in this model again falls slightly bluer than the data. This result is, however, a great improvement over previous gray atmosphere isochrones.

5. SELECTION OF CLUSTER MEMBERS

5.1. *Previous Estimations and Control Fields*

The most comprehensive study of NGC 2168's population (Barrado y Navascués et al. 2001b) used main-sequence counting techniques to discover ~1700 cluster members in their data. When combined with data from other studies (brighter stars), the total cluster mass, based on an average mass of 0.6 $M_\odot$, is estimated to be ~1600 $M_\odot$. Sung & Bessell (1999) used mass function integrations to also estimate a total mass of 1660 $M_\odot$ for the cluster, although only 640 $M_\odot$ of stars were counted in the study. An earlier dynamical study by Leonard & Merritt (1989) placed the total cluster mass anywhere between 1600 and 3200 $M_\odot$.

All of these photometric studies of NGC 2168 have suffered in establishing the true cluster population given observational limits due to its large size. The spatial extent of the cluster easily fills the areal coverage in most detectors, and hence there are no documented faint studies of a blank field offset by at least 1° from the core. Although there is a small effect in these studies that will underestimate the total cluster population because of missed stars near the edge of the cluster, the true population may actually be overestimated because of improper blank field subtraction. To try to get around this, Barrado y Navascués et al. (2001b) used a wide strip centered on the main-sequence locus and counted all stars within this envelope. Field star subtraction was then estimated by using counts of stars surrounding the main sequence. The filters chosen by Barrado, Navascués et al. (2001b) separate the disk stars from the cluster stars better than a $V, B-V$ CMD; however, their cluster luminosity function may still include some faint K- and M-type disk dwarfs.

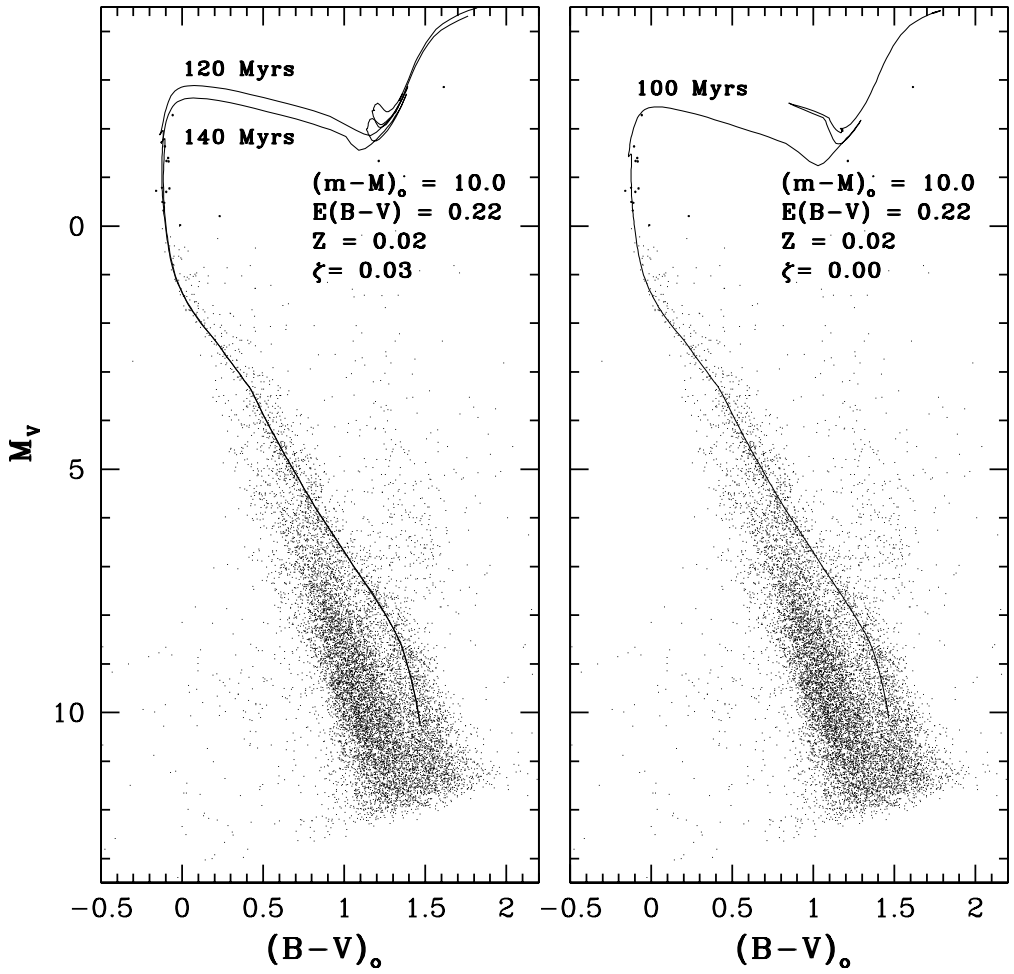

FIG. 4.—*Left*: Best-fit isochrones for NGC 2323 (age $\sim$ 130 Myr), based on a core-overshooting model. *Right*: An equivalent fit obtained from a non-overshooting model of 100 Myr. The general shape of the main sequence is matched well to the solar-metallicity isochrone. See § 4 for a discussion of these results.

In the study by Sung & Bessell (1999), the observed cluster luminosity function was extrapolated beyond $V \sim 17.5$ (mass function beyond $\sim$0.7 $M_{\odot}$) based on counts in the Pleiades cluster. However, as mentioned in their paper, this overestimates the contribution of low-mass stars since the Pleiades sample includes the low-mass dominated outer regions of the cluster, which are not detected by Sung & Bessell (1999). For the brighter stars, they used proper-motion selection (a better technique of getting cluster membership); however, for the fainter stars they adjusted zero-age main-sequence lines in different filters for reddening excesses and computed distances for individual objects. Objects with inconsistent distances are assumed to be disk stars and are thrown out.

In the work of Leonard & Merritt (1989), an age of 30 Myr was used to represent NGC 2168 (from the work of Vidal 1973), much lower than the value found in recent studies. Additionally, most of the mass in the Leonard & Merritt (1989) study resided in faint main-sequence stars that were beyond the proper-motion detections. Therefore, an extrapolation was used to integrate the mass function using a power-law slope beyond $\sim$1 $M_{\odot}$. Binary effects and mass segregation were ignored in the study.

Our study also suffers from a small enough field of view that a 1 : 1 cluster field equivalent blank field (in terms of areal coverage) cannot be established. However, rather than count stars over our entire mosaic, we have chosen to build a blank field from the extreme outer regions of our field (an area of 122 arcmin^2, outside of $R = 20'$ from the center of the cluster). This field is almost a factor of 8 smaller in areal coverage than our cluster field. At this radius, the CMD shows no evidence of a main sequence; however, some cluster stars are most likely still present as previous proper-motion studies have shown (see § 1). Current-generation instruments, such as MEGACAM on CFHT, will easily allow a deep blank field to be obtained around this cluster.

For NGC 2323, the only study investigating the luminosity function of the cluster is the $V \leq 14.5$ effort of Claria et al. (1998). They concluded with a lower limit on the cluster population of 109 members (285 $M_{\odot}$). In this case, our areal coverage is not only large enough to encompass almost the entire cluster ($R \sim 15'$) but also large enough so that an almost areal equivalent blank field can be built up from the outer CCDs on the mosaic.

5.2. *Luminosity and Mass Functions*

We define the cluster stars by first creating main-sequence fiducials [defined by clipping objects with $\Delta(B-V) \geq 3.5\ \sigma$ from the mean] after roughly isolating the cluster main sequence from the background distribution. This creates an

TABLE 2
CORRECTED CLUSTER STAR COUNTS AND COMPLETENESS

V (mag) (1)	N NGC 2168 (2)	N NGC 2323 (3)	COMPLETENESS (CLUSTER/BACKGROUND) (4)
9.0–10.0	5.0 ± 2.2	4.0 ± 2.0	1/1
10.0–11.0.....	32.0 ± 5.7	7.0 ± 2.6	1/1
11.0–12.0.....	33.4 ± 9.0	26.8 ± 6.4	1/1
12.0–13.0.....	46.5 ± 10.5	45.3 ± 8.2	1/1
13.0–14.0.....	73.0 ± 14.1	53.7 ± 10.0	1/1
14.0–15.0.....	83.5 ± 17.0	83.4 ± 14.4	1/1
15.0–16.0.....	93.5 ± 20.6	99.6 ± 20.0	1/1
16.0–17.0.....	76.8 ± 22.3	109.1 ± 23.5	1.02/1
17.0–18.0.....	55.0 ± 21.7	149.3 ± 23.0	1/1
18.0–19.0.....	81.9 ± 19.9	156.8 ± 26.7	1.03/1.02
19.0–20.0.....	176.6 ± 29.0	226.4 ± 34.5	1.08/1.05
20.0–21.0.....	162.4 ± 41.3	308.7 ± 49.3	1.13/1.09
21.0–22.0.....	52.1 ± 25.7	534.5 ± 75.6	1.21/1.16
22.0–23.0.....	...	259.7 ± 39.7	1.36/1.18

envelope around the fiducial based on the errors in the photometry (the envelope broadens out toward faint magnitudes), and stars are counted within this envelope, for both the cluster CMD and the background CMD. The observed cluster luminosity function is the difference between the counts in the two fields after accounting for the difference in area between the cluster and background fields.

Incompleteness corrections are handled by repeatedly introducing a number of artificial stars into the data images. The method used for this has been described in both Papers II and III, so we present only the results here. Table 2 shows the statistics for these tests in both the cluster and blank fields (ratio of number added to number recovered) in column (4). The incompleteness tests were carried out for the NGC 2168 data set, and the recovered results are used for both clusters. This method is believed to be reliable since both of these clusters were imaged for identical exposure times and exhibit similar crowding. The corrections found here are very similar to those determined for NGC 2099 in Paper III. To summarize, the completeness in the cluster field for main-sequence stars is found to be 73.5% at $V = 22.5$.

The final corrected star counts are found by multiplying the cluster and blank field counts by the incompleteness corrections from Table 2. The final luminosity functions for each cluster are tabulated in columns (2) and (3) of Table 2 (corrected for incompleteness). Figures 5 and 6 show the corresponding luminosity functions for NGC 2168 (*solid line*) and NGC 2323, respectively. For NGC 2168, the luminosity function rises until $M_V = 5$, and then dips down and rises again. Although this dip ($M_V \sim 7$) is most likely the result of poor statistics or cluster stars being subtracted off in the blank field and not physical, we do not rule out the latter. Many open cluster CMDs, such as all four that we have looked at in detail in our survey, appear to show fewer stars in a thin band of the lower main sequence near this magnitude. We do note that the luminosity function given by Barrado y Navascués et al. (2001b) does not show a dip at this magnitude (Fig. 5, *dashed line*). This was constructed by using the *I*-band luminosity function in Table 3 of Barrado y Navascués et al. (2001b) and correcting to V by using the empirical fiducial in Table 1 of that paper. For

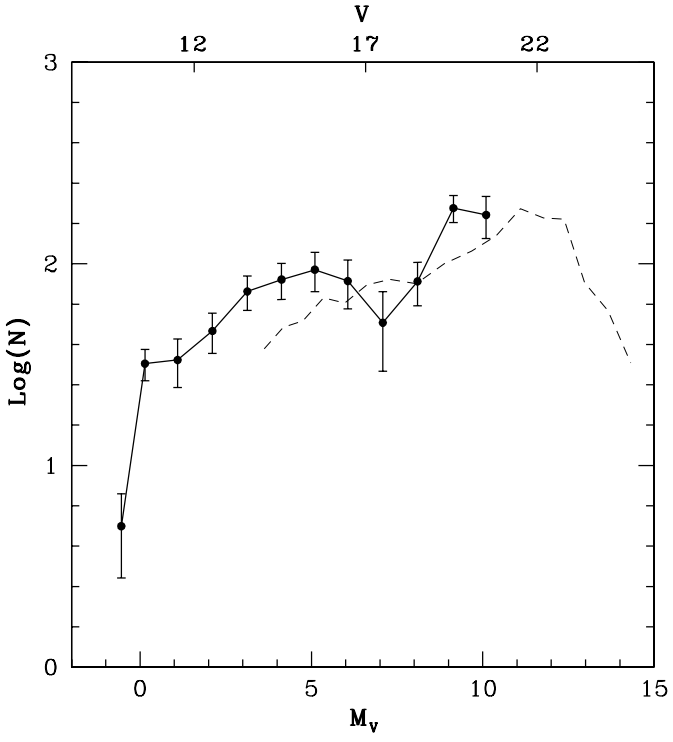

FIG. 5.—NGC 2168 luminosity function is shown before and after correcting for data incompleteness. The error bars reflect a combination of Poisson errors and incompleteness errors. The NGC 2168 luminosity function from Barrado y Navascués et al. (2001b) is also shown for comparison.

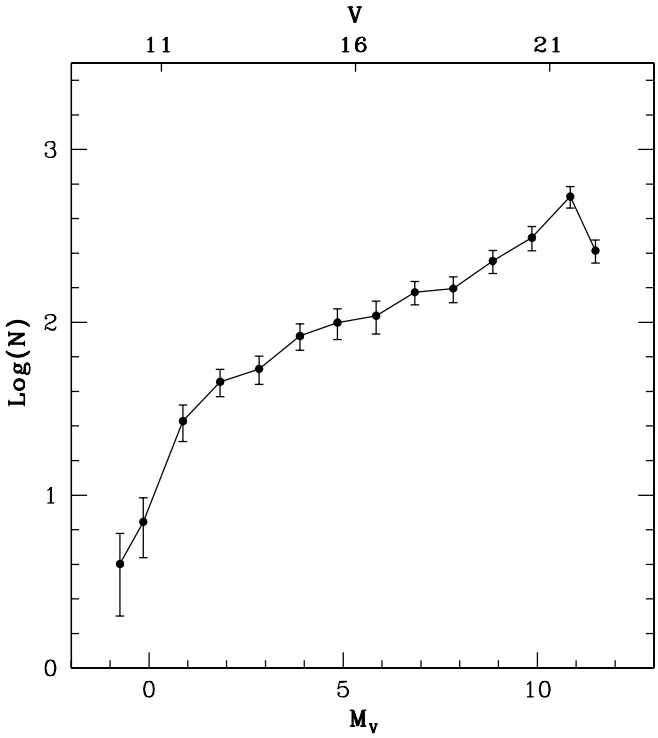

FIG. 6.—NGC 2323 luminosity function is shown after correcting for incompleteness. The luminosity function slowly rises up to $V \sim 21.5$ ($M_V = 10.82$). The error bars reflect a combination of Poisson errors and incompleteness errors.

NGC 2323, the luminosity function shows a steady climb up to the limit of our data where there is a small dip. Again, the last data point is likely affected by poor statistics. Both luminosity functions show a slow rise beyond $M_V \sim 8$. This rise is due to the change of slope in the mass-luminosity relation (see, e.g., D'Antona 1998) and may be seen as a change in slope of the cluster main sequence.

By summing the corrected luminosity function, we find a cluster population of just over 1000 stars down to $V \sim 22$ in the central 20′ of NGC 2168. The number of stars here has not been corrected for the chopped-off area on the north and south edges of the mosaic. Due to this, the effective area of this field is actually equivalent to a spherical 18′ field. Since our background field may contain some cluster stars, the above estimate is likely to be a lower limit. This number increases significantly when the cluster luminosity function is extended to the hydrogen-burning limit. For this, we normalize our luminosity function with respect to the Barrado y Navascués et al. (2001b) function and predict that there are ~500 additional stars between $V = 22$ and $V = 25$.

For NGC 2323, we detect ~2050 stars in the central 15′ and down to $V \sim 22$. Again, since our data does not extend to the lowest mass stars, we can use the well-known Pleiades luminosity function (Lee & Sung 1995) to estimate the total population down to $M_V = 15$. For this, we find that an additional 1150 faint stars would exist in the cluster, raising the total population to 3200.

Figure 7 compares the luminosity functions for both NGC 2168 and NGC 2323 with that of the solar neighborhood (Binney & Merrifield 1998), the Pleiades (Lee & Sung 1995), and the 520 Myr old rich cluster NGC 2099 (Paper III). Each of the functions have been normalized by the total number of stars and then shifted arbitrarily in the vertical direction. The clusters are presented in order of increasing age, with the Pleiades (the youngest) at the top of the diagram, directly beneath the solar-neighborhood luminosity function. It is clear that this data does not reach deep enough to see the turnover in the luminosity functions of NGC 2168 or NGC 2323 (the last data point in each function has been eliminated given the large error bar).

To compute the mass functions of these clusters, we multiply the observed luminosity functions by the slope of the mass-luminosity relationship (from the models). The resulting mass function is usually expressed as a power law,

$$\Psi(m) \propto m^{-(1+x)} , \quad (1)$$

where $x = 1.35$ represents the Salpeter value. For NGC 6819, we found a very flat mass function ($x = -0.15$). This was expected as the cluster is very old (10 times the dynamical relaxation time). For NGC 2099, the best-fit slope was found to be $x = 0.60$. Other studies, specifically Francic (1989), have shown that older clusters systematically show flatter mass functions. This is believed to be due to the preferential loss of low-mass stars, a consequence of dynamical evolution toward energy equipartition.

The mass functions of NGC 2168 and NGC 2323 are presented in Figures 8 and 9. Fitting a slope to the global NGC 2168 mass function gives a value of $x = 1.29 \pm 0.27$, almost identical to the Salpeter slope. Our result splits the values found in previous studies; Leonard & Merritt (1989) found $x = 1.68$ for the extreme high-mass end of the cluster mass function, Sung & Bessell (1999) found a flatter value of $x = 1.1$, and Barrado y Navascués et al. (2001b) found $x = 1.59$ for 0.8–6 $M_\odot$. For NGC 2323, we find $x = 1.94 \pm 0.15$ over the mass range 0.40–3.90 $M_\odot$. No previous estimates exist in the literature. Therefore, for the four clusters that we have already looked at in the CFHT Open Star Cluster Survey, the mass function is found to be systematically steeper as the cluster age decreases.

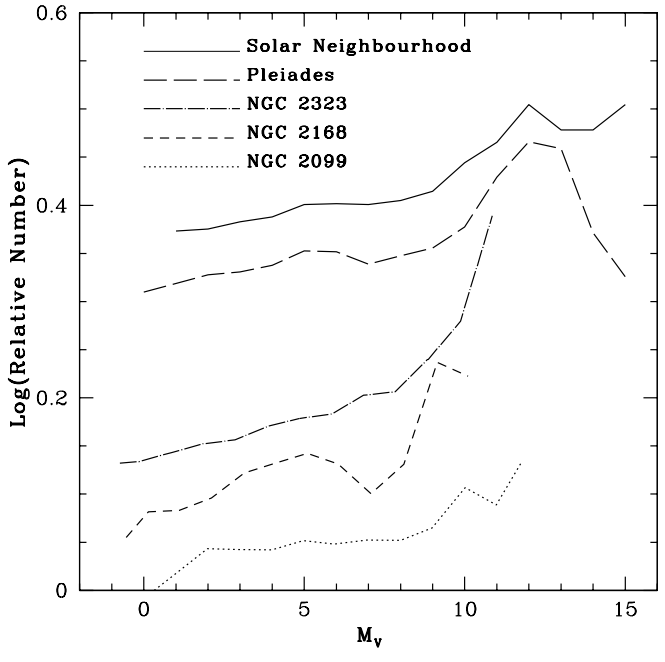

FIG. 7.—Luminosity functions of NGC 2168 and NGC 2323 are compared with those of the solar neighborhood, the Pleiades, and NGC 2099. Each luminosity function has been normalized by the total number of stars and then scaled up arbitrarily. The clusters are shown in terms of increasing age, with the Pleiades being the youngest at the top, under the solar neighborhood.

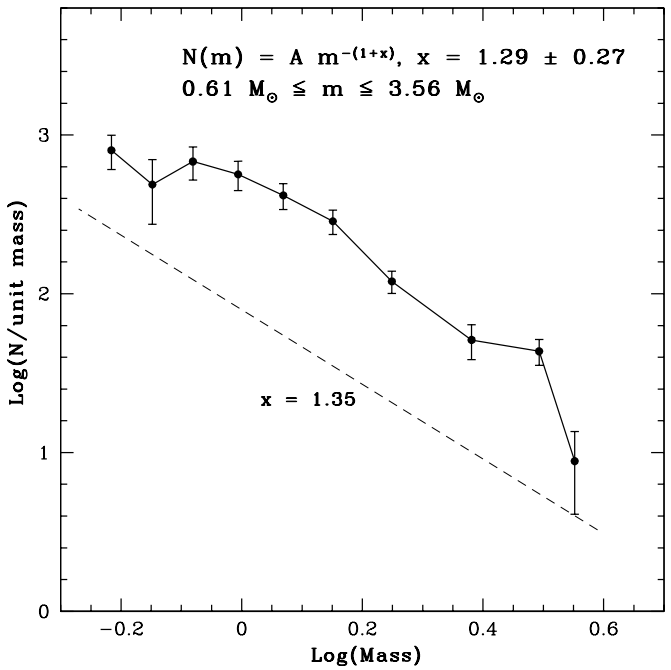

FIG. 8.—NGC 2168 global ($R < 20'$) mass function ($x = 1.29 \pm 0.27$, *solid line*) is found to be almost identical to a Salpeter IMF ($x = 1.35$, *dashed line*).

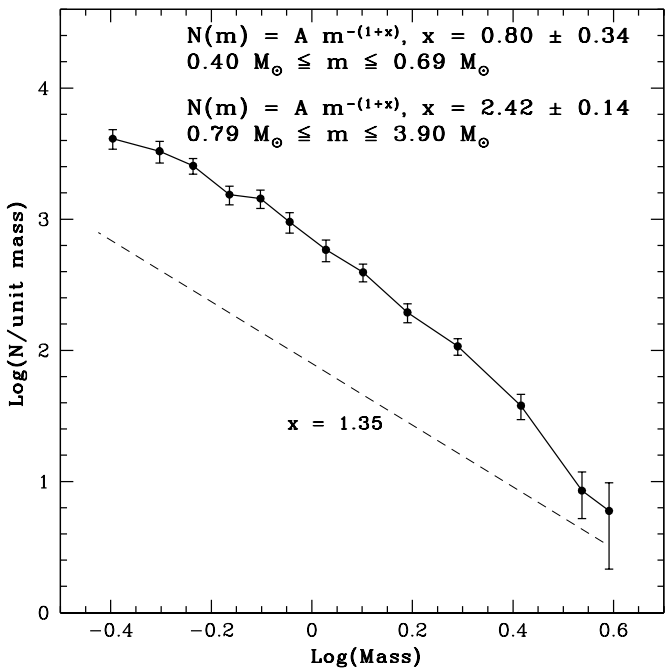

FIG. 9.—NGC 2323 global ($R < 15'$) mass function ($x = 1.94 \pm 0.15$, *solid line*) is found to be steeper than a Salpeter IMF ($x = 1.35$, *dashed line*).

5.2.1. *Dynamical State and Mass Segregation*

As mentioned earlier, young open star clusters are excellent test cases to determine the IMF as they represent a group of stars with a similar age and composition. However, this IMF can be determined only if the cluster has retained the stellar population that it was born with; that population has not suffered from preferential mass loss. This mass loss occurs as the cluster relaxes toward a state of energy equipartition due to distant two-body interactions between all the stars within the cluster. In an equilibrium state, the lower mass stars will be moving with a higher velocity and therefore will be more likely found in the outskirts of the cluster. There, they are preferentially lost from the cluster tidal boundary. Thus, dynamical relaxation leads to mass segregation, manifested by a systematic change in the slope of the local mass function with radius, and to an evolution of the global cluster IMF, generally from a relatively steep slope (a high value of x) to a smaller slope, with time. If we can show that there is no evidence of this dynamically induced mass segregation, then there is hope for setting constraints on the IMF. If, however, we find that dynamical effects have shifted the stellar distribution, then these dynamical effects can still lead to an important understanding of the timescales and levels of mass segregation in clusters. The caveat is that we must disentangle dynamical evolution from primordial mass segregation, a process that may be inherent in cloud collapse to begin with.

Binney & Tremaine (1987) characterize the dynamical relaxation time in terms of the number of crossings of a star that are required for its velocity to change by order of itself,

$$t_{\rm relax} \sim t_{\rm cross} \frac{N}{8 \ln N} , \qquad (2)$$

where N is the total number of stars. Using our distance and apparent size of NGC 2168, we estimate that the dynamical relaxation age is 111 Myr, which implies that the cluster age is 1.6 times its relaxation age. For NGC 2323, the dynamical age is 102 Myr, which gives a cluster age of less than 1.3 times the relaxation age.

TABLE 3
GEOMETRY OF ANNULI

Annulus	Radius (arcmin)	Radius (pixels)
NGC 2168:		
A1	$0 \le R < 5$	$0 \le R < 1456$
A2	$5 \le R < 10$	$1456 \le R < 2912$
A3	$10 \le R < 15$	$2912 \le R < 4369$
A4	$15 \le R < 20$	$4369 \le R < 5825$
Global	$0 \le R < 20$	$0 \le R < 5825$
NGC 2323:		
A1	$0 \le R < 3$	$0 \le R < 873$
A2	$3 \le R < 7$	$873 \le R < 2039$
A3	$7 \le R < 11$	$2039 \le R < 3204$
A4	$11 \le R < 15$	$3204 \le R < 4368$
Global	$0 \le R < 15$	$0 \le R < 4368$

To investigate signs of mass segregation, we split the clusters into four annuli (with geometry given in Table 3), and present mass functions in each annulus in Figures 10 and 11. Note that each annulus with a radius greater than $\sim 14'$ is cut off horizontally at the top and bottom due to the edges of CFH12K (which are 14.′06 from the center of the mosaic). The results show that mass segregation is most likely present in both clusters. The outer annuli have steeper mass functions, indicating more lower mass stars relative to higher mass ones. Surprisingly, the effect is much more prominent in the younger NGC 2323, for which the mass function slope goes from $x = 2.74 \pm 0.40$ in the outer annuli ($11' \le R < 15'$) to $x = 0.82 \pm 0.27$ in the innermost annuli ($0' \le R < 3'$). For NGC 2168, the mass function slope

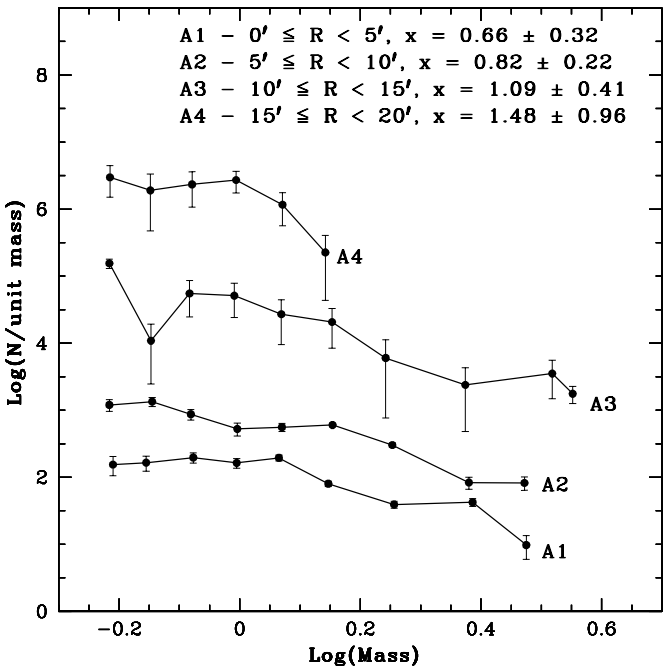

FIG. 10.—Mass functions in different annuli for NGC 2168 show mild evidence of mass segregation (steeper mass function in the outer rings) in the cluster.

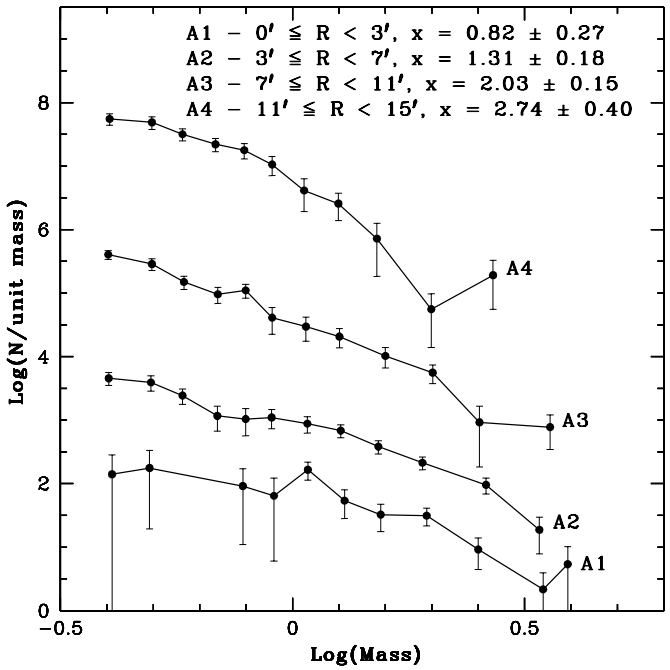

FIG. 11.—Mass functions in different annuli for NGC 2323 show clear evidence for mass segregation (steeper mass function in the outer rings) in the cluster despite its age being only 1.3 times the dynamical relaxation age.

changes from $x = 1.48 \pm 0.96$ in the outer annuli ($15' \leq R < 20'$) to $x = 0.66 \pm 0.32$ in the innermost annuli ($0' \leq R < 5'$).

As mentioned earlier, the mild mass segregation that we see in these young clusters could be primordial. Different clusters themselves may form with different concentrations of high-mass stars in the core and low-mass stars in the halo. This type of initial mass segregation has been observed in extremely young open clusters (Zinnecker & McCaughrean 1994), where the clusters are younger than the estimated relaxation timescales. Formation scenarios for these young clusters stress that the rapidity and efficiency of star formation is crucial in determining the final distribution of the stars (Battinelli & Capuzzo-Dolcetta 1991). Supernovae and stellar winds from the first generation of stars can effectively blow away remaining gas in the system to make the cluster unstable. The subsequent dynamical evolution of the cluster will be affected by the timescales and stages of this gas removal (Stecklum 1989). As for the IMF, it too depends on the local conditions of cloud collapse. For example, the final slope of the IMF will depend on how many cloudlets formed protostellar cores through collisions before the gravitational influence of the collapse ceased to be important (Murray & Lin 1996). Since the collisional frequency of the cloudlets will be greatest in higher density regions, such as the centers of clusters, more massive stars will also preferentially form in the center. This leads to a natural mass segregation within the cluster.

We can resolve these two cases of mass segregation induced either from dynamical evolution or primordial mass segregation by looking for signs of energy equipartition. Generally, dynamical mass segregation can be demonstrated if stars of different masses obey the radial distributions predicted by multimass King models (Gunn & Griffin 1979). This will be investigated for a series of clusters in a forth-coming paper.

6. WHITE DWARFS

The overall goal of our survey is to first identify white dwarf candidates in open star clusters and then obtain spectra to determine their masses. This will help us understand both the upper mass limit to white dwarf production and the initial-final mass relationship, which is a critical input for calculating ages from white dwarf cooling. The upper mass limit is also important in chemical evolution models of galaxies as it sets the lower mass limit for Type II supernovae. White dwarfs in NGC 2168 and NGC 2323 represent the most important sample in this study since they constrain the high-mass end of the relationship. With core-overshooting main-sequence turnoff masses of $\sim 5\ M_{\odot}$, some white dwarfs in both of these clusters are expected to have massive progenitors.

Our photometry for these clusters is deep enough to detect the faintest white dwarfs, which could have cooled during the lifetime of the clusters. Based on the cluster ages, we expect the faintest white dwarfs (assuming $1.0\ M_{\odot}$ objects) in both clusters to be located at $V \sim 22$. The younger age of NGC 2323 pushes this limit to a brighter magnitude; however, the larger distance modulus has an opposing effect. The combination of small number statistics in the faint blue end of the CMDs and much smaller blank fields does not allow us to build white dwarf luminosity functions. We will however attempt an estimation of the field white dwarf numbers by scaling up the blank field numbers to the area of the cluster field and also by using the Galactic disk white dwarf luminosity functions (Leggett, Ruiz, & Bergeron 1998). Previously, the only white dwarfs spectroscopically confirmed in either of these clusters are the two objects measured by Reimers & Koester (1988) in

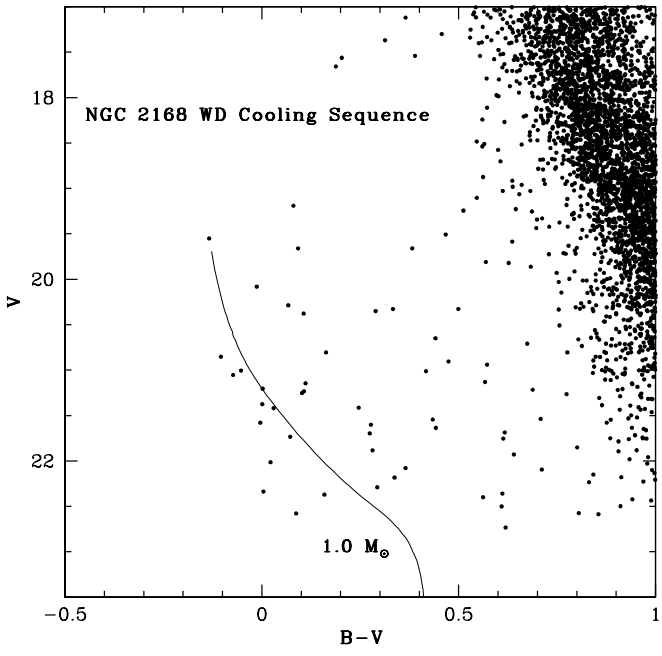

FIG. 12.—A $1.0\ M_{\odot}$ white dwarf cooling sequence (Wood 1994) is shown with respect to the potential white dwarfs in NGC 2168. The clump of objects located at $21 \leq V \leq 22$, $-0.15 \leq B-V \leq 0.1$ falls slightly fainter than the cooling model, indicating perhaps an even higher mass for these objects. The white dwarf cooling age from the faintest of these stars is found to be 190 Myr and therefore is in excellent agreement with the main-sequence turnoff age (180 Myr).

NGC 2168. We believe that further spectroscopy of new candidates in the present photometry of this cluster will yield more objects. The cleaned CMDs (removal of galaxies and image defects, see § 3) do show some concentrations of objects. For example, a clump of objects can be seen in NGC 2168 between $21 \leq V \leq 22.5$, $B-V = 0$. For NGC 2323 more of a scattered distribution of objects is seen in the white dwarf region.

We can predict the number of expected white dwarfs in each of these clusters by integrating the main-sequence mass functions from the present-day turnoff mass to the upper limit for white dwarfs production. For the latter, our models show $M_{\rm up} \sim 7\ M_{\odot}$; however, the value could be as low as 5.5 $M_{\odot}$ (Jeffries 1997). The calculation of the number of expected white dwarfs assumes that the observed mass function shape is similar to that for the higher masses that have evolved off the main sequence. Given both the range of masses represented by the present-day mass functions (NGC 2323: 0.4–3.9 $M_{\odot}$), and the smoothness of the data, only a mild extrapolation to higher masses is needed for these young clusters. For NGC 2168, we use the mass function slope from 0.83 to 3.56 $M_{\odot}$ ($x = 1.75$) to estimate 18 expected white dwarfs in our cluster field. For NGC 2323, the mass function slope from 0.79 to 3.90 $M_{\odot}$ ($x = 2.42$) predicts six white dwarfs in the cluster.

Before we can compare the number of white dwarfs seen to the number expected, we must first remove the number of field white dwarfs (assuming galaxies have already been removed through the stellarity cut). For this, we use the disk white dwarf luminosity function (Leggett et al. 1998) and scale the number to our field of view. Since the Galactic disk is much older than these two clusters, we must truncate the counts in the field at the bright magnitudes that are represented by the white dwarf cooling limits of the clusters. For the NGC 2168 field, the disk white dwarf luminosity function predicts four white dwarfs down to $V = 22$. For NGC 2323, three field white dwarfs are predicted in the cluster field of view down to $V = 22$ (12 are predicted down to the limiting magnitude). The number of objects seen in the blank field after scaling up the counts given the smaller field of views are greater than these numbers. Counting objects on the CMD and eliminating these blank field numbers gives 14.5 white dwarfs in NGC 2168, after accounting for incompleteness errors. This number is in excellent agreement with the 18 estimated from the mass function extrapolation. For NGC 2323, five white dwarfs are found after the statistical subtraction and six were predicted. Although we do not know which of the objects on our CMD are cluster white dwarfs, we now have candidates for multiobject spectroscopic observations in these two clusters.

In Figure 12, we show a 1 $M_{\odot}$ cooling model (Wood 1994) with respect to the clump of potential white dwarfs in NGC 2168. The best white dwarf candidates are the eight objects clustered together in the range $21 \leq V \leq 22$, $-0.15 \leq B-V \leq 0.1$. These are all found to be slightly fainter than this cooling sequence, suggesting perhaps an even higher mass and therefore a potentially very important constraint on the white dwarf initial-final mass relationship and upper mass limit to production. For the 1 $M_{\odot}$ model, the corresponding white dwarf cooling ages for these objects range from 30 to 190 Myr. These values are in excellent agreement with the expected white dwarf cooling ages from stars which have evolved off the main sequence in this young cluster. Therefore, if the clump of objects in NGC 2168 are bona fide cluster white dwarfs, then we can conclude that the white dwarf cooling age of the cluster (190 Myr) is in good agreement with the main-sequence turnoff age

TABLE 4
SUMMARY OF RESULTS FOR NGC 2168

Parameter	NGC 2168
Position:	
α_{J2000}, R.A.	$06^{h}08^{m}54\overset{s}{.}0$
δ_{J2000}, decl.	$+24^{\circ}20\overset{\prime}{.}0$
l_{J2000}, Galactic longitude	$186\overset{\circ}{.}58$
b_{J2000}, Galactic latitude	$2\overset{\circ}{.}18$
Distance and reddening:	
$(m-M)_V$, apparent distance modulus	10.42
$E(B-V)$, reddening	0.20
A_V, visual extinction	0.62
$(m-M)_0$, true distance modulus	9.80
d, distance from the Sun (pc)	$912\ ^{+70}_{-65}$
z, distance above Galactic plane (pc)	36.6
Age:	
$t_{\rm Dynamical}$, dynamical relaxation timescale (Myr)	111
$t_{\rm Isochrone}$, main-sequence turnoff age (Myr)	180
$t_{\rm WD}$, white dwarf cooling age (Myr)	$\sim$190
Metallicity:	
Z, heavy-metal abundance[a]	0.012
Size:	
D, linear diameter (pc)	10.6
Θ, angular diameter (arcmin)	40
N, number of stars down to $M_V = 15$	$\sim$1500[b]
Stellar distribution:	
α, mass function slope (Salpeter = 2.35)	2.29 ± 0.27

[a] These values were not spectroscopically determined.
[b] Our study does not include the entire cluster.

TABLE 5
SUMMARY OF RESULTS FOR NGC 2323

Parameter	NGC 2323
Position:	
α_{J2000}, R.A.	$07^{h}02^{m}48\overset{s}{.}0$
δ_{J2000}, decl.	$-08^{\circ}22\prime 36\prime\prime$
l_{J2000}, Galactic longitude	$221\overset{\circ}{.}67$
b_{J2000}, Galactic latitude	$-1\overset{\circ}{.}24$
Distance and reddening:	
$(m-M)_V$, apparent distance modulus	10.68
$E(B-V)$, reddening	0.22
A_V, visual extinction	0.68
$(m-M)_0$, true distance modulus	10.0
d, distance from the Sun (pc)	$1000\ ^{+81}_{-75}$
z, distance above Galactic plane (pc)	22.7
Age:	
$t_{\rm Dynamical}$, dynamical relaxation timescale (Myr)	102
$t_{\rm Isochrone}$, main-sequence turnoff age (Myr)	130
$t_{\rm WD}$, white dwarf cooling age (Myr)	...
Metallicity:	
Z, heavy-metal abundance[a]	0.020
Size:	
D, linear diameter (pc)	8.72
Θ, angular diameter (arcmin)	30
N, number of stars down to $M_V = 15$	$\sim$3200
Stellar distribution:	
α, mass function slope (Salpeter = 2.35)	2.94 ± 0.15

[a] These values were not spectroscopically determined.

(180 Myr). For the former age, we would also need to add ~50 Myr for the main-sequence lifetime of a progenitor 7 $M_{\odot}$ star before making any comparisons.

7. CONCLUSION

Deep photometry of NGC 2168 and NGC 2323 in the V and B filters has allowed us to produce the tightest main sequences to date for these clusters. NGC 2168 is found to contain ~1000 stars brighter than $V = 22$, beyond which we can not reliably trust the luminosity function. In NGC 2323 we find ~2050 stars above the photometric limit of $V \sim 23$. After accounting for uncertainties in the reddening, main-sequence fitting, extinction, and metallicity, the distance to NGC 2168 is determined to be 912^{+70}_{-65} pc. For NGC 2323, we find $d = 1000^{+81}_{-75}$ pc. By comparing a new set of theoretical isochrones to the observational CMDs, we have determined the ages of both clusters (180 Myr for NGC 2168 and 130 Myr for NGC 2323) and also found a nice agreement between the theoretical isochrone and the observational main sequence. Both clusters are found to exhibit mild signs of mass segregation. The global mass function of NGC 2168 is found to have a slope of $x = 1.29$, almost identical to a Salpeter IMF ($x = 1.35$). For NGC 2323, we found $x = 1.94$, steeper than the Salpeter value. Spectroscopic confirmation of potential white dwarfs in both clusters are important for setting high-mass constraints on the initial-final mass relationship. Summaries of the overall results for both NGC 2168 and NGC 2323 are given in Tables 4 and 5, respectively.

J. S. K. received financial support during this work through research grants PGS-A and PGS-B from the Natural Sciences and Engineering Research Council (NSERC) of Canada. H. B. R. and G. G. F. are supported in part by NSERC. H. B. R. extends his appreciation to the Killam Foundation and the Canada Council for the award of a Canada Council Killam Fellowship.

REFERENCES

Barbaro, G., Dallaporta, N., & Fabris, G. 1969, Ap&SS, 3, 123
Barrado y Navascués, D., Deliyannis, C. P., & Stauffer, J. R. 2001a, ApJ, 549, 452
Barrado y Navascues, D., Stauffer, J. R., Bouvier, J., & Martin, E. L. 2001b, ApJ, 546, 1006
Battinelli, P., & Capuzzo-Dolcetta, R. 1991, MNRAS, 249, 76
Becker, W., & Fenkart, R. P. 1971, A&AS, 4, 241
Bertelli, G., Bressan, A., Chiosi, C., Fagotto, F., & Nasi, E. 1994, A&AS, 106, 275
Bertin, E., & Arnouts, S. 1996, A&AS, 117, 393
Bessell, M. S., Castelli, F., & Plez, B. 1998, A&A, 333, 231
Binney, J., & Merrifield, M. 1998, Galactic Astronomy (Princeton: Princeton Univ. Press)
Binney, J., & Tremaine, S. 1987, Galactic Dynamics (Princeton: Princeton Univ. Press)
Canuto, V. M., & Mazzitelli, I. 1992, ApJ, 389, 724
Castellani, V., Degl'Innocenti, S., & Prada Moroni, P. G. 2001, MNRAS, 320, 66
Claria, J. J., Piatti, A. E., & Lapasset, E. 1998, A&AS, 128, 131
Collinder, P. 1931, Ann. Obs. Lund, 2, 1
Cudworth, K. M. 1971, AJ, 76, 475
Cuffey, J. 1938, Ann. Astron. Obs. Harvard Coll., 106, 39
———. 1941, ApJ, 94, 55
D'Antona, F. 1998, in ASP Conf. Ser. 142, The Stellar Initial Mass Function, ed. G. Gillmore & D. Howell (San Francisco: ASP), 157
de Bruijne, J. H. J., Hoogerwerf, R., & de Zeeuw, P. T. 2001, A&A, 367, 111
Deliyannis, C. P., Barrado y Navascués, D., & Stauffer, J. R. 2000, BAAS, 32, 41.08
Deliyannis, C. P., & Steinhauer, A. 2001, BAAS, 33, 42.03
Deliyannis, C. P., et al. 2003, in preparation
Ebbighausen, E. G. 1942, AJ, 50, 1
Francic, S. P. 1989, AJ, 98, 888
Gunn, J. E., & Griffin, R. F. 1979, AJ, 84, 752
Hauschildt, P. H., Allard, F., & Baron, E. 1999, ApJ, 512, 377
Hersperger, T. 1973, A&A, 22, 195
Hoag, A. A., Johnson, H. L., Iriarte, B., Mitchell, R. I., Hallam, K. L., & Sharpless, S. 1961, Publ. US Naval Obs., 2d Ser., Vol. 17 (Washington: US Naval Obs.) 347
Jeffries, R. D. 1997, MNRAS, 288, 585
Johnson, M. L., Hoag, A. A., Iriarte, B., Mitchell, R. I., & Hallam, K. L. 1961, Lowell Obs. Bull., 5, 8
Kalirai, J. S., et al. 2001a, AJ, 122, 257 (Paper I)
———. 2001b, AJ, 122, 266 (Paper II)
Kalirai, J. S., Ventura, P., Richer, H. B., Fahlman, G. G., D'Antona, F., & Marconi, G. 2001c, AJ, 122, 3239 (Paper III)
Landolt, A. U. 1992, AJ, 104, 340
Lee, S., & Sung, H. 1995, J. Korean Astron. Soc., 28, 45
Leggett, S. K., Ruiz, M. T., & Bergeron, P. 1998, ApJ, 497, 294
Leonard, P. J. T., & Merritt, D. 1989, ApJ, 339, 195
McNamara, B. J., & Sekiguchi, K. 1986a, ApJ, 310, 613
———. 1986b, AJ, 91, 557
Meurers, J., & Schwarz, A. 1960, Veröff. Univ. Sternw. Bonn, No. 53
Mostafa, A. A., Hassan, S. M., Aiad, A., & Ahmed, T. 1983, Astron. Soc. Egypt, 5, 23
Murray, S. D., & Lin, D. N. C. 1996, ApJ, 467, 728
Rieke, C. A. 1935, Circ. Harvard College Obs., No. 397
Reimers, D., & Koester, D. 1988, A&A, 202, 77
Sarrazine, A. R., Steinhauer, A. J. B., Deliyannis, C. P., Sarajedini, A., Bailyn, C. D., Kozhurina-Platais, V., von Hippel, T., & Platais, I. 2000, A&AS, 32, 742
Shapley, H. 1930, Star Clusters, Appendix B (New York: McGraw-Hill)
Smart, W. M. 1925, MNRAS, 85, 257
Stecklum, J. B. 1989, Astron. Nachr., 310, 375
Sung, H., & Bessell, M. S. 1999, MNRAS, 306, 361
Sung, H., & Lee, S.-W. 1992, J. Korean Astron. Soc., 25, 91
Topaktas, L. 1975, A&AS, 20, 269
Trumpler, R. 1930, Lick Obs. Bull., 420, 154
Ventura, P., Zeppieri, A., Mazzitelli, I., & D'Antona, F. 1998, A&A, 334, 953
Vidal, N. V. 1973, A&AS, 11, 93
von Hippel, T., Kozhurina-Platais, V., Platais, I., Demarque, P., & Sarajedini, A. 2000, in ASP Conf. Ser. 198, Stellar Clusters and Associations, Convection, Rotation and Dynamos, ed. R. Pallavicini, G. Micela, & S. Sciortino (San Francisco: ASP), 75
von Hippel, T., Steinhauer, A., Sarajedini, A., & Deliyannis, C. P. 2002, AJ, 124, 1555
Wood, M. A. 1994, BAAS, 26, 1382
Zinnecker, H., & McCaughrean, M. J. 1994, Infrared Phys. Technol., 35, 569